Mesoscopic simulations of hydrophilic cross-linked polycarbonate polyurethane networks

Soft Matter

PAPER

View Article Online
View Journal | View Issue

Cite this: *Soft Matter*, 2016, 12, 5029

Mesoscopic simulations of hydrophilic cross-linked polycarbonate polyurethane networks: structure and morphology†

E. Iype,[a] A. C. C. Esteves[a] and G. de With*[b]

Received 11th March 2016,
Accepted 3rd May 2016

DOI: 10.1039/c6sm00621c

www.rsc.org/softmatter

Polyurethane (PU) cross-linked networks are frequently used in biomedical and marine applications, *e.g.*, as hydrophilic polymer coatings with antifouling or low-friction properties and have been reported to exhibit characteristic phase separation between soft and hard segments. Understanding this phase-separation behavior is critical to design novel hydrophilic polymer coatings. However, most of the studies on the structure and morphology of cross-linked coatings are experimental, which only assess the phase separation *via* indirect methods. Herein we present a mesoscopic simulation study of the network characteristics of model hydrophilic polymer networks, consisting of PU with and without methyl-polyethylene glycol (mPEG) dangling chains. The systems are analyzed using a number of tools, such as the radial distribution function, the cross-link point density distribution and the Voronoi volume distribution (of the cross-linking points). The combined results show that the cross-linked networks without dangling chains are rather homogeneous but contain a small amount of clustering of cross-linker molecules. A clear phase separation is observed when introducing the dangling chains. In spite of that, the amount of cross-linker molecules connected to dangling chains only, *i.e.*, not connected to the main network, is relatively small, leading to about 3 wt% extractables. Thus, these cross-linked polymers consist of a phase-separated, yet highly connected network. This study provides valuable guidelines towards new self-healing hydrophilic coatings based on the molecular design of cross-linked networks in direct contact with water or aqueous fluids, *e.g.*, as anti-fouling self-repairing coatings for marine applications.

1. Introduction

Polyurethanes (PUs) are amongst the most used industrial polymers and find applications in many different technological fields, such as flexible foams, (hydrophilic) coatings, sealants, composites, electric and magnetic materials.[1] Cross-linked PU networks are of particular interest as their thermal and mechanical properties can be easily tuned, by using different chemical structures, from the very large range of raw materials available, or by varying the formulation ratios and synthesis conditions. Understanding how these networks are formed is critical to design novel hydrophilic polymer coatings.

PU cross-linked networks are normally composed of a "soft" segment, typically consisting of polyols, and a relatively "hard" segment, formed by the reaction between multifunctional isocyanates and the polyols (or polyamines) which act as chain extenders.[2,3] The hard segment often comprises the cross-linking points, which will largely determine the structural arrangements of the network and final properties of the material. Furthermore, depending on the composition of the different polymer blocks and segments in the network, the cross-linking density and the network topology, PUs can range from soft elastomers to rather hard thermoplastics.

It has been reported that the combination of soft and hard segments in PUs can lead to clearly phase-separated structures,[2] typically with a "matrix" of the flexible domains embedding the hard domains. The hard segments can form strongly aggregated phases due the polarity and hydrogen bonding of the urethane bonds, but if the cohesion force between these segments is not strong enough, the cross-linked PUs may be composed of partially miscible phases.[3] Furthermore, other strong physical interactions, like crystallization of the hard segments which act as "pseudo" cross-links for the soft phase, can also lead to large phase separated domains. In extreme cases, this phase separation has great implications on the final "bulk" and surface properties of the material.

The introduction of dangling chains into cross-linked PUs, which can be seen as "imperfections" in the network, can also

[a] *Laboratory of Physical Chemistry, Department of Chemical Engineering and Chemistry, Eindhoven University of Technology, Eindhoven, The Netherlands*
[b] *Laboratory of Materials and Interface Chemistry, Department of Chemical Engineering and Chemistry, Eindhoven University of Technology, Eindhoven, The Netherlands. E-mail: G.deWith@tue.nl*

† Electronic supplementary information (ESI) available. See DOI: 10.1039/c6sm00621c

strongly affect the morphology and materials properties. Depending on their chemical characteristics (molecular weight, polarity, *etc.*), concentration in the network and in which segment they are incorporated, dangling chains may have a large influence on the molecular dynamics of PUs.[2,4] When introduced into the soft segment, they can act as plasticizers reducing considerably the polymer rigidity and, hence, decrease the glass transition temperature T_g of the PU.[5] On the other hand, when incorporated as chain extenders in the hard segment, although the hydrogen bonds between the urethane groups still dominate the molecular dynamics, the molecular relaxations can be strongly affected, depending on the chemical nature and content of the imperfections in the network.[6,7]

Most of the investigations performed on the morphology of PU networks, including the study of the influence of dangling chains, have been based on experimental techniques only.[8–13] Small angle X-ray scattering (SAXS),[9] Infrared (IR) spectroscopy[10] and thermal characterization techniques[11] have been largely used to study segmented polyurethane block copolymers, and evaluate different aspects related to, either the chemical and physical interactions between the soft and hard phase, or the phase-domain characteristics, such as average inter-domain size, degree of phase separation or interfacial domain thickness. Seymour *et al.*[12,13] used differential scanning calorimetry (DSC) and IR spectroscopy to identify the presence of a clear phase separation in a series of polyurethane block polymers, which was mainly governed by the short- and long-range ordering of the hard segments, rather than the hydrogen-bonds dissociation, as reported for the large majority of the studies on phase separated PUs. Huh *et al.*[8] combined X-Ray and DSC techniques and observed two major transition regimes, attributed to the presence of the ester/ether soft segments and the aromatic-urethane hard segments, which were assigned to specific molecular mechanisms of relaxation. These relaxation phenomena were greatly influenced by the molecular weight of the polymers, the weight percentage of the hard segments and the thermal history of the materials. Optical (OM) and electron (EM) microscopy have also been extensively applied on the study of segmented PU to investigate their morphology. Chen *et al.*[14] reported macroscopic phase separation in model polyurethane networks, mostly caused by incompatibilities present in the reacting polyurethane mixtures, in spite of the use of the largely compatible pre-polymers polypropylene oxide (PPO) and ethylene oxide (EO). Finally, transmission electron microscopy (TEM) and atomic force microscopy (AFM) have also allowed elucidation of the microphase-separated structure of PUs at nanoscale level.[15]

In spite of all this, experimental molecular information on these networks is scarcely available. Moreover, computer simulation approaches, in spite of their high potential to study the morphology and network structure of such polymer systems at a molecular (nano) and/or meso-scale level, have been rather limitedly explored for this purpose as well. Recently, Dissipative Particle Dynamics (DPD) simulations were used to create the cross-linked structure of an epoxy resin[16,17] and infer about its materials properties, such as elastic modulus, glass temperature transition and thermal expansion coefficients.[18] A few simulation-based works are reported in the literature for similar PU networks for hydrophobic coatings.[19–21] One of this papers reports the presence of clustering of the dangling chains within the PU network.[19] However, neither the amount and nature of clustering was fully quantified, nor could the experiments confirm or negate such a phenomenon.

In the current work we use a simulation approach, based on a DPD method, to study hydrophilic polyurethane networks, which could find applications as functional coatings in the marine or biomedical fields, due to their anti-fouling,[22] low-lubricity or anti-bacteria properties. Since these functionalities rely mostly on the surface chemical composition, the presence of the hydrophilic groups at the surface is crucial. This can be achieved by introducing hydrophilic dangling chains in the cross-linked networks, which will spontaneously segregate towards the surface, typically in contact with water or aqueous media, providing the required functionalities to the coated materials. This strategy is also supported by previous reports showing the self-orientation of dangling chains towards the surface on polyester polyurethane cross-linked networks.[19,21] This phenomenon is particularly interesting to develop self-replenishing coatings,[20,21] in which the performance, *i.e.*, surface functionality of the materials, can be maintained at a high level throughout an extended life-time *via* the continuous self-reorientation of the functional dangling chains towards new surfaces, created after the occurrence of damage.

Our systems are based on polycarbonate (PC) polyol pre-polymers, reacted with a tri-isocyanate to form a cross-linked PU network. The hydrophilic dangling chains inserted in the network are methyl-polyethylene glycol (mPEG) polymers of low molecular weight. The network structures and morphology were analyzed using a number of tools, such as the radial distribution function, cross-link density distribution and Voronoi volume distribution (of the cross-linking points). The study of the network characteristics, such as the cross-linking conversion of systems prepared with sub- and super-stoichiometric ratios and the distribution of the cross-linking points, revealed details of the network structure, while the study of the morphology of the systems with and without dangling chains disclose extreme differences in what concerns phase-separation phenomena and the creation of heterogeneous networks.

2. Simulation details

2.1 Creating cross-linked systems: dissipative particle dynamics (DPD)

In this work dissipative particle dynamics (DPD) is used to study the morphology of polycarbonate based networks, both with and without mPEG (Fig. 1) as hydrophilic dangling chain. DPD is a coarse-grained simulation method in which coarse-grained entities, the ''beads'', represent parts of a molecule, which interact with each other. In dissipative particle dynamics the total force acting on each bead j is

$$f_j = f_j^{\mathrm{C}} + f_j^{\mathrm{D}} + f_j^{\mathrm{R}} \quad (1)$$

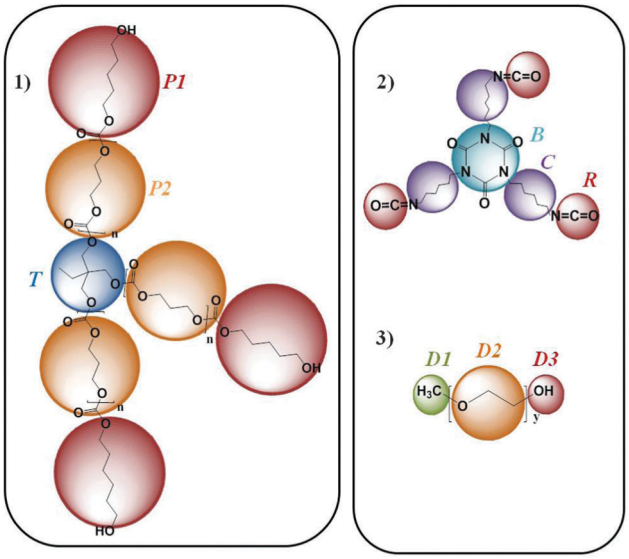

Fig. 1 Individual components of the polyurethane networks: (1) polycarbonate (PC_{3n} with n = 7 the number of carbonate repeating units per arm, P2-beads), (2) tri-isocyanate cross-linker and (3) polyethylene glycol ($mPEG_y$) dangling chains, y = 45 with y the total number of EG ethylene glycol units (D2-beads). The chemical structures and bead representations as used in simulations are shown. The volume of the beads is just indicative of the different sizes, but not to scale in terms of the real volume used. P1, R and D3-beads represent the "reactive" groups building up the cross-linked network.

where the superscripts indicate conservative, dissipative, and random forces, respectively. The dissipative and random forces are coupled by a fluctuation–dissipation relation and determine the thermalization of the system.[25] The coefficients of friction are adapted from the work of Groot and Warren.[23] In addition, all DPD forces are sums of pair interactions that obey Newton's third law, and therefore, momentum is conserved. This gives rise to the correct hydrodynamic behavior at larger length and time scales.[24] The equilibrium structure is determined by the conservative forces. The total conservative potential of DPD is a sum of bonded and the non-bonded terms. We use stretch and bending potentials for the bonded terms.[26] The non-bonded potential between two beads i and j with interaction parameter a_{ij} is soft, short-ranged, and purely repulsive and follows the expression

$$V_{\mathrm{DPD},ij}(r_{ij}) = \frac{a_{ij}}{2}\left(1 - \frac{r_{ij}}{L_{\mathrm{DPD}}}\right)^2 \quad \text{for}$$
$$r_{ij} < L_{\mathrm{DPD}} \text{ and } V_{\mathrm{DPD},ij}(r_{ij}) = 0 \text{ for } r_{ij} \geq L_{\mathrm{DPD}} \qquad (2)$$

where r_{ij} is the distance between beads i and j, and L_{DPD} is the nonbonded interaction cutoff, which is taken to be the same for all bead types. The nonbonded polymer bead interactions are calculated as a sum of two parts: a neutral interaction $\hat{a}_{ij}$ term and a pairwise interactions part proportional to the Flory–Huggins parameter χ_{ij}, which quantifies how much beads dislike each other. Previously,[16] we have established the following generalized relation to compute like–like interactions as

$$a_{jj} = (P - \rho_{j,\mathrm{pure}} kT)/(\alpha \rho_{j,\mathrm{pure}}{}^2 L_{\mathrm{DPD}}{}^3) \qquad (3)$$

where a_{jj} is the like–like interaction parameter, $\rho_{j,\mathrm{pure}}$ indicates the pure-liquid number density of bead j, P is the set pressure, and α is a constant in the DPD equation-of-state, which is equal to 0.101 for number densities higher than 3.25. These parameters are chosen such that, at their experimental pure liquid densities, a liquid consisting of beads of solely type i has the same pressure as a liquid of j beads. This will give different a_{jj} values for beads having different pure-liquid densities.

To compute pairwise interactions, a scaling relationship is derived[16] to couple thermodynamic properties to DPD parameters between beads having variable molar volumes.

$$a_{ij} = \hat{a}_{ij} + \frac{P\chi_{ij}}{0.0454\left(a_{ii}\rho_i^{\mathrm{pure}} + a_{jj}\rho_j^{\mathrm{pure}}\right)} \text{ and } \hat{a}_{ij} = \sqrt{a_{ii}a_{jj}} \qquad (4)$$

The range of the interaction can easily be calculated[16] for use in eqn (2). For the present simulations we thus applied the same parametrization, which allows for variable bead volumes,[16] as used before.

The repulsion parameter a_{ij} for each bead pair is calculated from solubility parameters of the beads, which in turn are calculated using the van Krevelen method.[27] These parameters correspond well with the results of molecular dynamics calculations performed using the COMPASS force field. The simulation is performed under reduced units with a DPD length unit corresponding to $L_{\mathrm{DPD}} \approx$ 7.2 Å and equivalent DPD time unit corresponding to ≈8.3 ps. The time scale is chosen so that the thermal (root mean square) bead velocity is 1 (in DPD units where L_{DPD} = 1).

The systems chosen for analysis consist of a mixture of a polycarbonate-based polymer (PC) and a tri-isocyanate cross-linker (tHDI), with or without methyl-polyethylene glycol dangling chains (mPEG). The chemical formulae of each of the components and the equivalent bead representations as used in the simulations are shown in Fig. 1. Three sub-stoichiometric mixtures with polymer (P1-beads) in relation to cross-linker (R-beads) (1.5 : 1, 1.25 : 1, 1.1 : 1), three super-stoichiometric mixtures with excess of cross-linker in relation to polymer (1 : 1.1, 1 : 1.25, 1 : 1.5) and the stoichiometric mixture (1 : 1) were chosen for analysis. The system with mPEG dangling chains was chosen at a stoichiometric ratio (1 : 1) of polymer + mPEG (P1- + D3-beads)to cross-linker (R-beads), as well as with two off-stoichiometric values, namely super-stoichiometric 1 : 1.25 and sub-stoichiometric 1.25 : 1.

The details for each system are given in Table 1. The number of polymer molecules was kept constant in all the mixtures. Since the size of cross-linker molecule is smaller, changing the number of cross-linker molecules did not influence significantly the overall system size. The LAMMPS program was used for all simulations.[28] Each mixture was inserted in simulation boxes with sizes in accordance with a desired number density of $3.0 L_{\mathrm{DPD}}{}^{-3}$. Initially the systems were energy minimized and then equilibrated using constant *NVT* conditions. Equilibration was judged by the convergence of the energy as a function of DPD simulation time before cross-linking, using typically 50 000 time steps. Further, the polymer (and the dangling chains) and cross-linker molecules were allowed to react, *i.e.*, to cross-link, when their distance is smaller than a preset value.

Table 1 System configurations used in the simulations. The number of polymer and cross-linker molecules used for each mixture are given. The B-bead density is calculated by dividing the number of B-beads by the volume of the simulation box

Mixtures (polymer to cross-linker ratio)	Polymer molecules	Cross-linker molecules	Dangling chains	Box side length (DPD units)	B-bead number density
1 : 1.5	4000	6000	—	36.17	0.126
1 : 1.25	4000	5000	—	35.57	0.111
1 : 1.1	4000	4400	—	35.19	0.101
1 : 1	4000	4000	—	34.94	0.093
1.1 : 1	4000	3636	—	34.70	0.087
1.25 : 1	4000	3200	—	34.42	0.078
1.5 : 1	4000	2666	—	34.07	0.067
1 : 1.25-DC	5565	7729	1855	45.48	0.082
1 : 1-DC	5565	6183	1855	44.99	0.067
1.25 : 1-DC	5565	4946	1855	44.41	0.056

It has been shown that the resulting structure is relatively insensitive to details of the cross-linking process.[16,29] Here the preset value for establishing a cross-link was chosen to be 0.4 DPD units. Note that all reactions are done within the DPD framework according to a previously established procedure[16,19] and that MD simulations are only carried out to obtain proper parameters for use in DPD.

2.2 Parameterization of pair interactions, bonds and angles

The bond length and bond angle interactions between beads were parameterized by performing full atom molecular dynamics (MD) simulations of the respective molecular fragments using the COMPASS force field at constant *NPT* conditions (for details, see the ESI,† SI-1). Although the MD simulations are done for monomers, the effect of density differences will be taken into account by the DPD procedure used, that was specifically designed to take density effects into account.[16–18] The COMPASS force field was used as this force field has been shown to be rather effective in connection with polymer molecules. The resulting configurations were used for coarse-graining and extracting the bond and valence angle parameters and are shown in Tables S1 and S2 (ESI†), respectively. In addition to bond interactions, the parameterization of pair interactions was done based on previous work which takes into account variable bead volumes.[16] A list of the pair interaction parameters is given in SI-2, Table S3 (ESI†). The pair interaction parameters slightly change depending on the changes in the number of molecules for different systems. This is because in this formulation, the average bead volume is a parameter, on which the interaction parameters depend, and which varies somewhat with composition. The force constants for bond angle bending are much smaller than the force constants for bond stretching. Thus bond angles are significantly more flexible than bond distances. In addition, all the equilibrium values for bond angles are close to 90 degrees, thus ensuring the non-linearity of valence angles and thereby introducing coiling of polymer chains.

2.3 Cross-linking conversion and density calculations

Cross-linking is defined as the process of establishing a connection between the ''reactive'' P1-beads in the polymer and R-beads in the cross-linker and occurs when the distance between the beads are less than 0.4 DPD units (see Section 2.1). At every time step, the program searches for possible connections based on this distance criterion and permanent connections are established if this condition is satisfied. The cross-linking conversion is calculated by taking the ratio of newly formed connections at every step divided by the maximum number of possible connections due to cross-linking.

2.4 Cross-linking point RDF, Voronoi volume and density distribution

The radial distribution function (RDF) is a common tool to characterize molecular systems. Here it is used to analyze the cross-linked network and in this case, the ''particles'' are the cross-linking points (B-beads). The radial distribution is calculated by taking the pairwise distance distribution of ''particles'' within the system, normalized, as usual, by taking its value at large distance to be equal to one. The RDF of the cross-linking points provides a characteristic of the network structure in terms of distances while the area under the peaks multiplied by the number density yields the coordination number of ''particles'' in the consecutive coordination shells. Structure factors for the B-bead distributions were calculated as well but did not reveal any extra information on their spatial distribution. Therefore, we focused on the RDFs.

For a set of cross-linking points, Voronoi diagrams[30–32] can be drawn in which each cell corresponding to a cross-linking point represents the locus of points which are closer to that cross-linking point than to any other. Once the cell is constructed, the volume of such a cell can be calculated. Thus for each cross-linking point, there is a corresponding Voronoi volume. The Voronoi volume distribution (VVD) is characteristic of the network structure. If this distribution obeys a log normal type function, then all the points are homogeneously distributed in the network.[32] In this work, the Voronoi volume is calculated by creating a convex hull around the mid points between a ''particle'' and its neighbors, and then counting the volume using tetrahedral integration using the software Scientific Python Package. To check the quality of the Voronoi tessellation we checked a model system consisting of 1–1 PC–tHDI without mPEG chains using the Voronoi volume for all beads in a single frame against the Voro++ software, which showed excellent agreement. We used the Python software because in this package it is easy to loop over several frames

to take an average, while this is less straightforward in the Voro++ software.

The distribution of cross-linking points over space was calculated to study the morphology of the cross-linked network. If this distribution obeys a normal distribution, then all the points are homogenously distributed within the network, according to the central limit theorem. The cross-linking point density distribution (CPDD) was calculated by creating grids within the simulation box, calculating the number of cross-linking points associated with each grid point and plotting a normalized probability histogram for the number of cross-linking (B) beads. The results obtained are largely independent of the grid size used.

In all these three types of calculations, at least 1000 configurations from the DPD simulations were used so that the statistical fluctuations are minimized. All the RDF, VVD and CPDD calculations were made on cross-linked systems at the final conversion obtained, unless stated otherwise.

3. Results and discussion

3.1 Cross-linked polyurethane networks without dangling chains

3.1.1 Cross-linking conversion at different stoichiometric ratios. Fig. 2 shows the cross-linking conversion as a function of reaction time for all the systems without dangling chains. The curves show the systems in which different stoichiometric ratios of polymer to cross-linker molecules were used in the initial mixture. The sub-stoichiometric ratios had an excess of polymer (1.5 : 1, 1.25 : 1, 1.1 : 1) and the super-stoichiometric ratios had an excess of cross-linker (1 : 1.5, 1 : 1.25, 1 : 1.1). The stoichiometric system with an equal number of polymer and cross-linker molecules (1 : 1) is also given for comparison. The cross-linking conversion was calculated based on the minority component. As can be seen from Fig. 2, most of the systems achieved a final conversion of more than 97.5% after 60×10^3 DPD time units, but there are differences in the reaction kinetics according to the stoichiometry of the initial mixtures. In the inset, a magnified section is shown in order to assess the rate of conversion for each of these mixtures. It can be seen that the stoichiometric mixture (1 : 1) is the slowest in terms of cross-linking rate while all the off-stoichiometric mixtures are faster. Additionally, the cross-linking rate, defined as the maximum slope of the curve, is proportional to the degree of deviation from the stoichiometric mixture (see Fig. S1, ESI†). This implies that the mixtures with the highest degree of deviation from the stoichiometric mixture, *i.e.*, sub-stoichiometric (1.5 : 1) and super-stoichiometric (1 : 1.5), show the fastest cross-linking rate compared to the other off-stoichiometric mixtures. This is true for all the systems in increasing order of deviation from stoichiometry. Between the mixtures with equal deviation from stoichiometry in terms of polymer or cross-linker, only negligible differences in the cross-linking kinetics are present. For instance, the systems 1.1 : 1 and 1 : 1.1 show similar kinetics, and this is true for all such combinations. This overall behavior appears to be consistent with classical chemical kinetics for 2nd order reactions,[33] although one would expect proper 2nd order behavior to apply for homogeneous systems, which are obtained only after (partial) cross-linking.

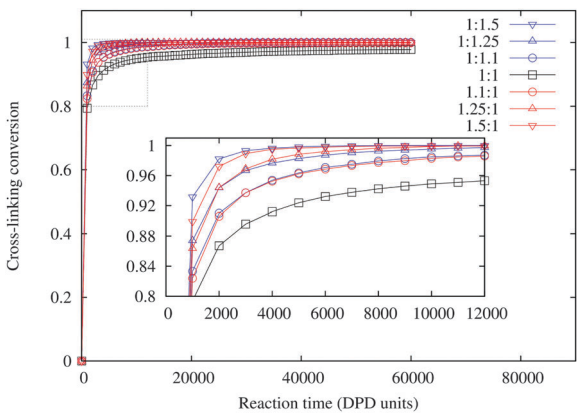

Fig. 2 Cross-linking conversion (based on the number of connections between R- and P1-beads) as a function of reaction time. Cross-linked systems obtained from mixtures with stoichiometric and various off-stoichiometric molar ratios are shown. The initial polymer to cross-linker ratios used in the mixtures are shown in the legend. The inset shows a detail of curves in the early times of reaction, to assess the reaction rates for the different mixtures.

3.1.2 Structure and morphology of the cross-linked network. Fig. 3 shows a snapshot of the final cross-linked structure for the stoichiometric mixture at final conversion. The red (dark) beads are the cross-linker molecules (beads B, C and R) and the white beads are polymer molecules (beads T, P1 and P2). From a visual inspection, the distribution of the cross-linker molecule beads seems rather homogeneous. Any indication of local clustering must be attributed to the grouping of individual beads of the cross-linker molecules (snapshots showing the center beads B of the cross-linker molecule in red and all other beads in white are shown in Fig. S2, ESI†). The distribution of the cross-linking points (*i.e.*, the location of the B-beads in the network) is of particular interest to detect any heterogeneity in the networks. In order to further characterize the distribution of B-beads in the cross-linked network, the RDFs, the VVDs and CPDDs were calculated.

At the end of the equilibration period the precursor and cross-linker molecules are more or less demixed (into droplets enriched in cross-linkers, see Fig. 3a). After cross-linking, though, both type of components are thoroughly mixed, as shown in Fig. 3b and c. Hence, the cross-linking reaction is having a significant effect on the microstructure, even in the absence of mPEG chains, and the cross-linking reaction ''compatibilizes'' the precursor and cross-linker molecules. This is due to the ''nature'' of the newly formed beads after cross-linking, which have an intermediate interaction strength value, thereby solubilizing the reacting mixture.

Radial distribution function (RDF). In order to assess the homogeneity of the network, we calculated the RDF for the cross-linking points (B-beads) for various stoichiometric systems with: (i) all beads completely free, (ii) all beads properly connected to molecules, (iii) all beads properly connected to molecules and

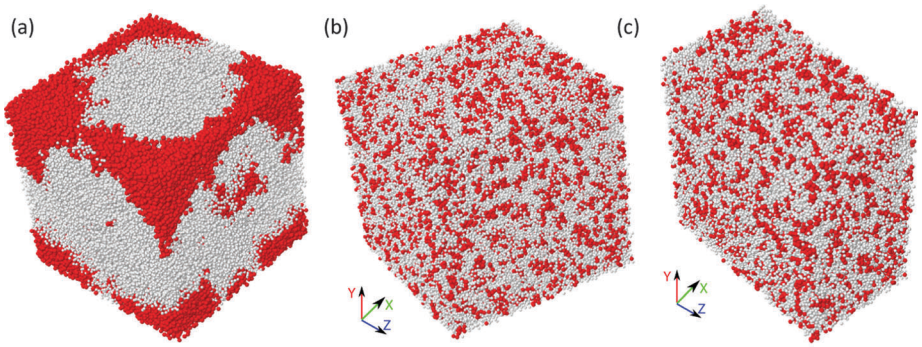

Fig. 3 Snapshots of the structures for the stoichiometric system (1 : 1) without dangling chains. (a) After equilibration, but before cross-linking showing the complete simulation box of $35 \times 35 \times 35 L_{DPD}^{3}$; (b) after cross-linking at final conversion; (c) cross-section of the same box as shown in (b) with size $15 \times 35 \times 35 L_{DPD}^{3}$. White beads: polymer precursor molecules and red (dark) beads: cross-linker molecules.

cross-linked and (iv) all beads connected to molecules and cross-linked but using a (number-weighted) average of all interactions instead of the proper interactions as reference. The results are shown in Fig. 4.

The first and second peak, represent the nearest and next nearest-neighboring B–B bead distance, respectively, *i.e.*, the first and second coordination shells, respectively. The peak position represents the (average) distance of the B beads while the area below the peak, when multiplied with the B-bead density ($0.093 L_{DPD}^{-3}$), corresponds to their coordination number (CN). For the various RDFs only minor shifts in the various peak positions are observed, while the areas below the peaks change considerably.

The first peak, representing the nearest-neighboring B-bead distances, is located at less than one DPD unit. One can expect, though, that the distance between B–B beads of two connected cross-linker molecules should be more than one DPD unit. In order to understand this, the RDF plots of all bead pairs in connected cross-linker molecules (BB, BC, BR, CC, CR and RR) are given in Fig. 5. Among all pairs, BC and CR are directly connected and therefore they both exhibit a significant first peak at around the bond distance ($\approx 0.7 L_{DPD}$ and $\approx 0.5 L_{DPD}$, respectively). Another, indirectly connected, pair is BR (1 to 3), which also shows a significant peak near its bonding distance, $\approx 0.9 L_{DPD}$. These first peaks also show the highest intensity while the peak heights of the remaining two non-connected bead pairs BB and CC are less intense (Fig. 5). This indicates that the first peak in Fig. 4 does not relate to the connected interactions but just shows a local ordering of the B-beads due to the overall pair interactions within the system. The stiffnesses of the angles, calculated using MD simulations (see Table S2, ESI†), are extremely low which makes the angles highly flexible and this is the reason that such a local ordering of non-connected beads within the system is possible. In order to put this in context, we note that a randomly arranged stoichiometric system with no pair interactions results in an average B–B bead distance of about 2.2 DPD units. This suggests that there exists a small amount of clustering of B-beads. From the peak position for the second coordination shell, $\approx 1.5 L_{DPD}$, it will be clear that the molecular chains between cross-linking points are highly coiled.

The calculated CNs, given in Table 2, decrease with increasing constraint, that is, from completely free *via* connected to molecules to connected to molecules and crosslinked. This also suggests that clustering will happen but less so with increasing constraint. To compare whether the B-beads cluster in the cross-linked state we compare the connected to chains and cross-linked RDF using the proper interactions with that of the

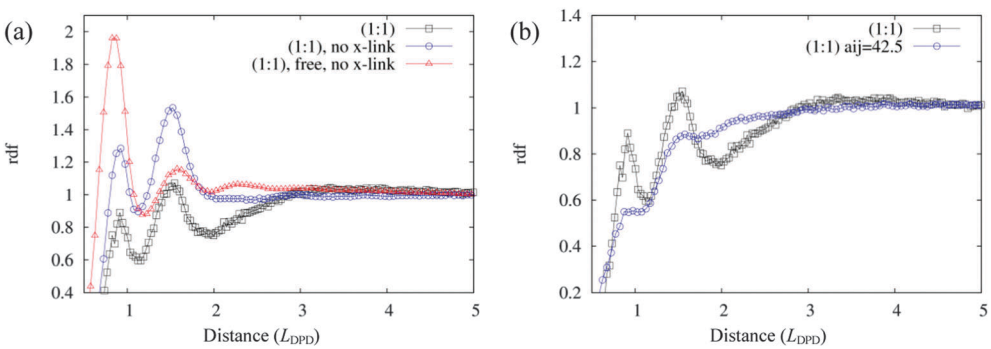

Fig. 4 (a) RDFs of the B-beads (cross-linking points) for stoichiometric systems in which: (i) the beads are completely free (free, no ×-link); (ii) all beads are connected to a molecule, but the molecules are not cross-linked (no ×-link), (iii) all the beads are connected to a molecule and cross-linked (1 : 1). (b) RDFs of the B-beads for stoichiometric systems with: (i) all beads connected to a molecule and using proper interactions (1 : 1) and (ii) all beads connected to a molecule and cross-linked using (number weighted) average interactions.

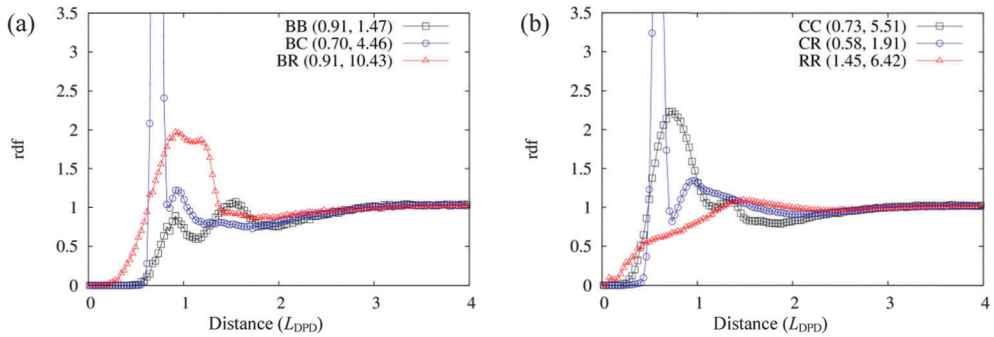

Fig. 5 RDFs of various bead pairs for the system cross-linked with stoichiometric ratio (1 : 1). (a) B–B, B–C and B–R RDFs; (b) C–C, C–R and R–R RDF. First peak heights (left) and areas under the curve (right) are given in the legend.

Table 2 Coordination numbers (CN) for the various stoichiometric systems

	CN1	CN2
Beads completely free using proper interaction	0.79	2.6
Beads connected to chains using proper interaction	0.49	3.2
Beads connected to chains and cross-linked using proper interaction	0.26	2.0
Beads connected to chains and cross-linked using average interaction	0.11	1.0

connected to chains and cross-linked RDF but with using (number weighted) average interactions. The ratio of the CN1s is about 2.4, which is indeed consistent with a relatively small amount of clustering. The ratio of the CN2s shows a similar trend. Note that, while the overall number density of all beads together is $3.0L_{DPD}^{-3}$, that of the B-beads is only $\cong 0.093\ L_{DPD}^{-3}$, resulting in the overall low CNs.

We also calculated the RDFs for the cross-linked super- and sub-stoichiometric systems. All these RDFs, shown in Fig. S3 (ESI†), show rather similar behavior to the RDF for the stoichiometric system. The peak positions and the area under the peaks of Fig. S3 (ESI†) for the various mixtures are provided in Table S1 (ESI†). The first CN does not show a systematic trend with composition, but fluctuates slightly around about its average value of 0.11, consistent with the value obtained for the stoichiometric system. It must be pointed out that the error margins (not shown for better clarity) for each of these curves are higher than the differences between the curves and, therefore, the small variations in the peak heights and areas arise from statistical fluctuations only. Overall, we conclude that for all systems, a small but significant amount of clustering of the cross-linking point (B-beads) is present.

Voronoi volume distribution (VVD). Fig. 6 shows the Voronoi volume distribution of the cross-linking points for stoichiometric and non-stoichiometric systems. It appears that all the curves follow a log-normal distribution. The peak heights (maxima) and the location of the maxima of the peaks (modes) are given as insets in this figure, and it can be seen that both change with stoichiometry. The maxima decrease as the polymer to cross-linker ratio increases, while the peak location moves to the higher values with increasing polymer to cross-linker ratio.

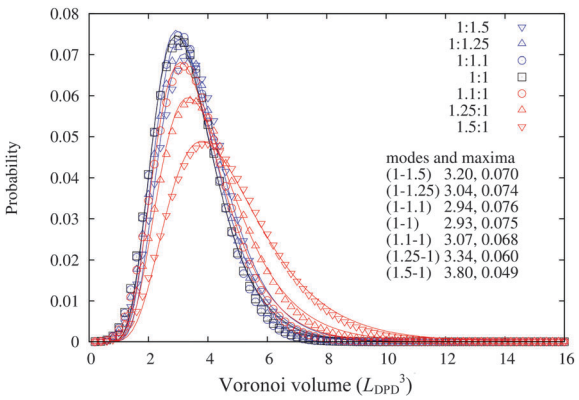

Fig. 6 Voronoi volume distributions (VVDs) of cross-linking points for systems with different stoichiometric ratios. The inset values are the modes (left) and maxima (right) of the peak for each of the systems. The lines indicate the fitted log-normal distribution.

This is consistent with the decrease in cross-linker density (*i.e.*, B-bead number density) with the increase of the polymer to cross-linker ratio, as shown in Table 1, *i.e.*, from sub- to super-stoichiometric ratios. The increase in peak height leads to a decrease in probability in the higher volume region. Thus one can see a cross-over somewhere near a volume of $5L_{DPD}^3$ in the figure. However, the presence of some clustering of the cross-linking (B) beads as derived from the RDFs is not recognizable in the VVDs.

Cross-linking point density distribution (CPDD). The CPDD is measured by creating a grid within the simulation box and counting the number of cross-linking points within each cell associated with a grid point. The probability for the number of cross-linking points is shown in Fig. 7a for systems cross-linked at super-stoichiometric ratios and Fig. 7b for sub-stoichiometric ratios. The black curve (cross label) in both figures shows the stoichiometric mixture. All the distributions in Fig. 7 are fitted with a (normalized) Gaussian distribution with the position x at the mean value and width σ given in the legend. From these data, it is clear that all the curves obey a Gaussian distribution quite closely.

The peak heights shifts from left to right as the polymer to cross-linker ratio decreases. This is expected as the cross-link

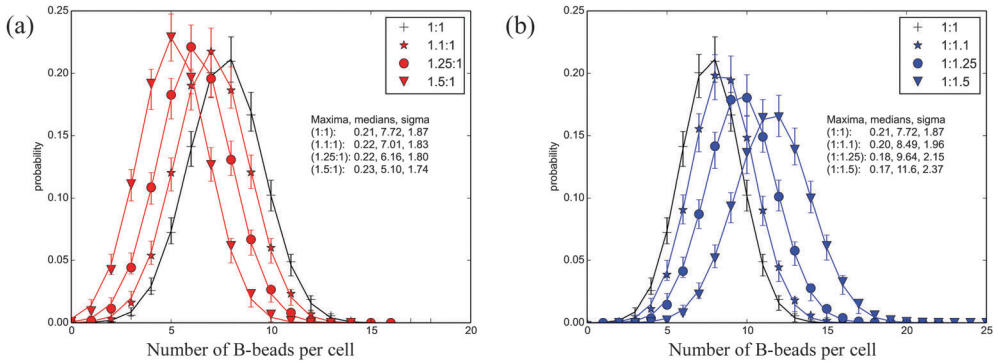

Fig. 7 Cross-linking point density distributions (CPDDs) in the networks as a function of number of B-beads per cell for the systems cross-linked with different stoichiometric ratios: (a) sub-stoichiometric and (b) super-stoichiometric compositions. The inset values correspond to the maximum (left) and median (right) of the peak for each of the systems. The lines are drawn to guide the eye.

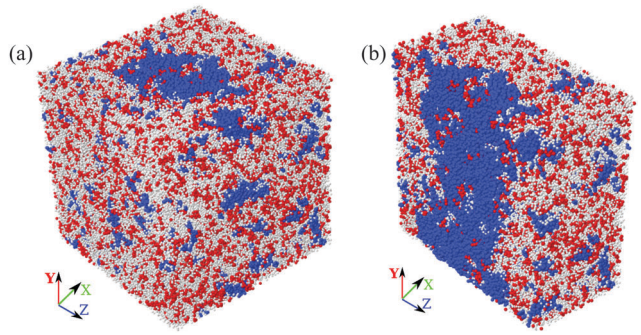

Fig. 8 Simulation snapshots of the cross-linked structures at final conversion for a stoichiometric system with mPEG dangling chains. Stoichiometric ratio of (1 : 1)-DC, (Table 1). (a) Complete simulation box of 45 × 45 × 45 (DPD units); (b) cross-section of the same box of 22 × 45 × 45 (DPD units). White beads = polymer precursor molecules, red beads = cross-linker molecules and blue beads = dangling chains.

density increases with decreasing polymer to cross-linker ratio. However, the changes in peak height are negligibly small compared to statistical errors. Moreover, also in the CPDDs the presence of clustering of cross-linking (B) beads as derived from the RDFs is not detectable.

In network theory as used, for example, for rubbers, a homogeneous distribution of the cross-link points and of the network chains between cross-links is normally assumed. The results of DPD simulations as analyzed by the RDFs show that some preferential clustering of the cross-link points occurs, which will possibly influence the chain length distribution between the cross-link points. However, in view of the absence, or actually rather limited presence, of inhomogeneity, we refrained from analyzing the chain length distributions.

3.2 Cross-linked polyurethane networks with PEG dangling chains

3.2.1 Distribution of the dangling chains in the networks. The structure of the cross-linked polyurethane system with mPEG chains is shown in Fig. 8. The system was energy minimized and equilibrated first, and then allowed to fully cross-link. A overall snapshot of the final system is shown in Fig. 8a, while a cross-section is shown in Fig. 8b for better visualization of the phase-separated regions. Corresponding images after equilibration but before cross-linking are shown in Fig. S4 (ESI†).

The white and red beads, from polymer and cross-linker molecules, respectively, appear to be intermixed as we have seen for the system without dangling chains (see Fig. 3). However, the blue beads (mPEG dangling chains) clearly form a phase-separated, cylinder-like region extending throughout the simulation box. Phase separation of dangling chains incorporated in polyurethane networks[2,4,34] and even the formation of "chemical clusters"[35] or specific surface-segregated domains,[19,36] have been widely reported in the literature, generally based on indirect experimental characterization methods, but as far as we know, has never visualized before with DPD simulations. The morphology of such phase-separated regions is expected to be highly dependent on the volume fraction and slightly dependent on the interaction strengths and may change from spherical *via* cylindrical to lamellar, as the volume fraction increases. As the interaction energy for a phase-separated mixture in DPD is proportional to the interface area between the phases, the box shape will influence the equilibrium shape of the domains as well. This effect was not investigated.

In order to understand the nature of this phase-separated region, we studied the density distribution of the mPEG dangling chains. Fig. 9a shows the cross-sectional density distribution of the mPEG-beads (D1, D2 and D3) at height $y = 20.5L_{DPD}$ of the simulation box (bottom: $y = 0$). Fig. S5 (ESI†) shows similar images for a range of y-values of the simulation box. From these images, it is clear that the phase-separated region extends throughout the simulation volume creating a cylinder-like phase-separated region. In case the mPEG2000 chains would be homogeneously distributed throughout the volume, the expected average number of mPEG-beads per cell associated with a sampling point is 19. Thus, the phase-separated regions were defined as the locus of 19 mPEG2000 beads per cell.

Apart from the continuous cylinder-like region, a number of small scattered phase-separated regions can be found in the volume considered (see, *e.g.*, the small clusters in the top half of Fig. 9a). The mPEG dangling chains are rather long ($\approx 22L_{DPD}$) but still reasonably compatible with the matrix and hence there

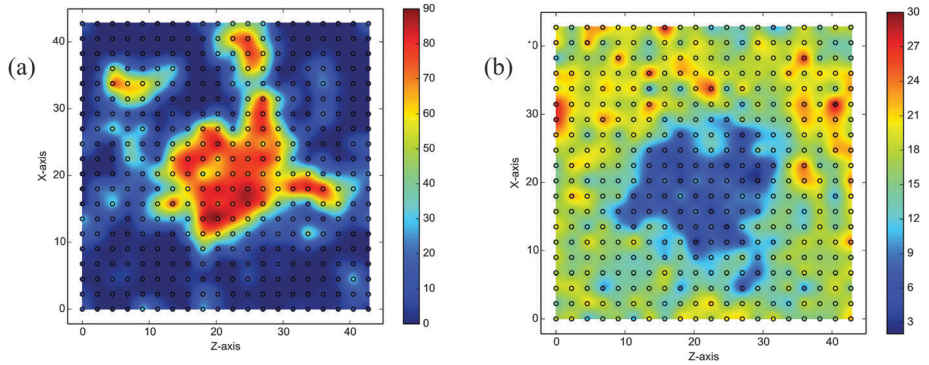

Fig. 9 Density distribution across the x–z plane of the mPEG structure at final conversion of the system at stoichiometric ratio (1 : 1-DC) (Table 1). (a) Cross-section at $y = 20.5L_{DPD}$ showing the mPEG dangling chain distribution. The color scale indicates the mPEG chain density per grid point; (b) projected cross-linking point (B-beads) distribution. The color scale indicates the cross-linking (B) bead density per grid point.

is a finite chance that they will also create smaller phase-separated domains where the cross-linker molecules are depleted. In order to see such depleted regions, the density distribution of the cross-linking points (B-beads) was calculated on the x–z plane for the total y-range, *i.e.*, the projected B-bead density, as shown in Fig. 9b.

The figure shows a depleted region in the middle of the simulation box where the cross-link (B-bead) density is lower compared to the rest of the plane. This raises the question whether all the mPEG2000 chains are cross-linked, *i.e.*, chemically bound, even though a high conversion is achieved for this system. Furthermore, we expect that the number of other components (non-mPEG2000) in these phase-separated regions is significantly lower, especially the number of cross-linker beads. For a cross-linked network, at least one arm of the cross-linker molecules must be connected to the polymer. Conversely, if the majority of the three arms of the cross-linker are connected to mPEG2000 chains only, a very weak and poorly bound network will be formed. To answer these questions, the fraction of cross-linker molecules connected to each of the other components was analyzed.

Table 3 shows the connection statistics (fraction of cross-linker molecules *versus* number of connections in the network) for the cross-linker molecules at final conversion. The first row shows the overall connectivity of the cross-linker. The zero value column implies that the cross-linker molecules are standalone, *i.e.*, not-connected to the network, and a value of three implies all the arms of the cross-linker are connected. It can be seen that the fraction of standalone cross-linker molecules is ≈2% and ≈84% of the cross-linkers have their three arms connected to either polymer or mPEG chains. For this 84% fully connected cross-linker molecules, a further analysis was done by calculating how many of those connections are to the polymer molecules *versus* to the dangling chains. Row 2 shows the fraction of cross-linkers with connections to the polymer molecules, while row 3 shows the fraction of cross-linkers connected to the dangling chains. From row 2 it can be seen that ≈80% of the fully connected cross-linkers have all their arms connected to polymers and ≈3% of the cross-linkers have none of their arms connected to the polymers, but instead to the dangling chains. The same distribution but in the reverse order is reflected by row 3. So, among the fully connected cross-linkers, only 3% have all their arms connected to mPEG chains and are not part of the main network. This seems to be a small fraction but there are also cross-linkers which are not fully connected (≈15%). A total of 270 (≈4%) cross-linkers is connected only to mPEG chains. This results in 458 out of the 1855 mPEG chains (≈25%) connected to the cross-linkers that do not form part of the main network. This is equivalent to about 3 wt% extractables in total.

Table 3 Percentage of cross-linker connections

Connectivity	0	1	2	3
Total connections of cross-linker (R-beads)	2	6	8	84
Connections to polymer beads (R-P1)	3	5	12	80
Connections to mPEG (R-D3)	80	12	5	3

3.2.2 Structure and morphology of the cross-linked networks with dangling chains. As discussed above, knowing that the majority of the mPEG dangling chains are connected to the network *via* the cross-linker molecules, and still form a rather significant separated phase, we investigated the structure and morphology of the cross-linked system containing the mPEG2000 dangling chains, with three mixtures with varying stoichiometric ratio of R-beads (super-stoichiometric 1 : 1.25, stoichiometric 1 : 1 and sub-stoichiometric 1.25 : 1). The number of individual molecules are given in Table 1 and the conversion is again close to 100%. The same methods used to analyze the cross-linked networks without dangling chains were also applied to this system, namely the radial distribution function (RDF), the Voronoi volume distribution (VVD) of the cross-linker points and the cross-link point density distribution (CPDD). The results are shown in Fig. 10.

The RDF shows two distinct peaks, similarly to what was observed for the systems without dangling chains (Fig. S3, ESI†), and the location of the peaks are also at similar distances, but the heights of the peaks are significantly different. The height of the first peak is larger than that of the second peak, contrary to the system without dangling chains. This is the result of more local clustering of B-beads from the cross-linker molecules for

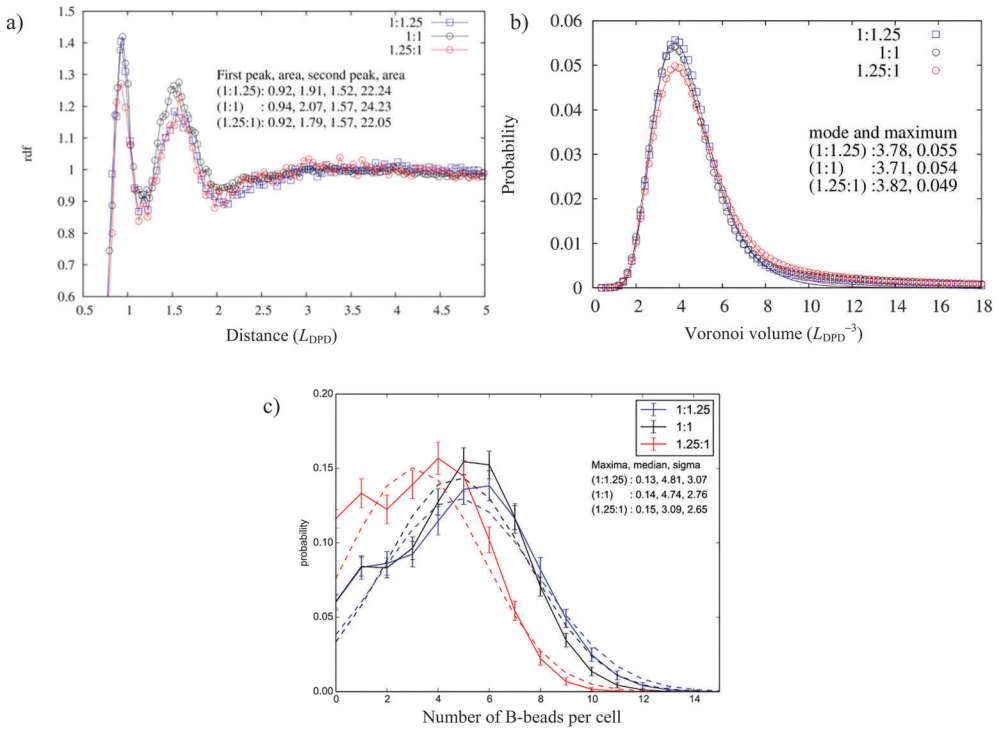

Fig. 10 RDFs, VVDs and CPDDs of the system containing mPEG dangling chains at final conversion obtained for super-stoichiometric (1 : 1.25), stoichiometric (1 : 1)-DC and sub-stoichiometric (1.25 : 1) composition. (a) The RDF of the cross-linking points; (b) the VVD of the cross-linking points; (c) the CPDD. For comparison with the stoichiometric system without dangling chains, see Fig. 4 (and Fig. S3, ESI†), Fig. 6 and 7, respectively.

the system containing dangling chains. The height of the second peak shows no significant change as compared to the system without dangling chains and among the various stoichiometric ratios and also the peak heights and locations do not show much variation. This confirms that varying the stoichiometry does not alter the morphology of the system significantly.

Also for the VVD similar results were obtained as for the system without dangling chains and the obey again a log-normal distribution with a trend in the change in mode and maxima of the distribution, consistent with that of the systems without dangling chains.

The CPDD, however, does not obey a Gaussian distribution, as was observed for the systems without dangling chains (Fig. 8). In all three mixtures there exists a shoulder at the left of the main peak in the distribution, indicating the deviation from a Gaussian distribution. This deviation shows that inhomogeneity and phase separation in the network, related to the phase separation of mPEG chains as observed for this system, is captured by the CPDD.

4. Conclusions

Studying the morphology of polyurethane (PU) based coatings is important to understand the nature and characteristics of such materials in order to better design and engineer products with enhanced properties. In view of the lack of in-depth understanding of the phase segregation occurring in PU networks, we investigated the behavior of such materials using computer simulation tools. In particular, we used a Dissipative Particle Dynamics (DPD) method, as recently extended to take a variable bead volume as well as cross-linking into account, to model polycarbonate-based PU cross-linked networks. Cross-linking was carried out using a previously established procedure.

The calculations were performed for systems with and without mPEG dangling chains. For the systems without dangling chains, mixtures with varying stoichiometric ratios between polymer and cross-linker molecules were studied. The cross-linked networks formed with these mixtures show no sign of phase separation. However, the radial distribution function indicates a limited local clustering of the cross-linker center beads. The Voronoi volume distribution of the cross-linking points and cross-link number density distribution do not show a significant deviation from the ideal log-normal or Gaussian distribution, respectively. Thus, we conclude that a small amount of clustering of cross-linker molecules occurs but that the extent of inhomogeneity in the distribution of cross-linking points in these networks is relatively small.

In contrast, the analysis of the system with dangling chains showed a significant amount of phase segregation. The mPEG2000 dangling chains self-segregated from the rest of the network, in spite of being largely connected to the cross-linker molecules as well as largely to the main network. Although the system has achieved nearly full conversion, the analysis of the connection statistics shows that there is a significant amount of mPEG chains ($\approx$25%) which are not part of the main network,

resulting in 3 wt% extractables (*i.e.*, non-network bonded species) in total. The segregation of the dangling chains from the rest of the network results in an inhomogeneous distribution of cross-linking points within the network in such a way that the regions where the dangling chains are present, are depleted of cross-linking points. This was also confirmed by the deviation of the cross-link distributions from a Gaussian distribution.

The results presented here will pave the way for a better understanding of the underlying network structure and further cement the foundation for the design of currently aspired self-replenishing hydrophilic coatings for marine and biomedical applications.

Acknowledgements

The authors thank the Ministry of Economic Affairs, Agriculture and Innovation *via* the IOP Self-Healing Materials programme (project #SHM012044) for funding and Ing. Leo van der Ven (Eindhoven University of Technology, NL) and Prof. Rolf van Benthem (DSM Ahead, Geleen, NL) for useful discussions.

References

1 (*a*) C. Hepburn, *Polyurethane Elastomers*, 2nd edn, Elsevier Applied Sciences, 1992; (*b*) G. Oertel, *Polyurethanes Handbook*, 2nd edn, Hanser, Munich, 1993.
2 Z. S. Petrovic and J. Ferguson, Polyurethane Elastomers, *Prog. Polym. Sci.*, 1991, **16**(5), 695–836.
3 L. L. Harrell, Segmented Polyurethanes. Properties as a Function of Segment Size and Distribution, *Macromolecules*, 1969, **2**(6), 607–612.
4 W. W. Yu, M. Du, D. Z. Zhang, Y. Lin and Q. Zheng, Influence of Dangling Chains on Molecular Dynamics of Polyurethanes, *Macromolecules*, 2013, **46**(18), 7341–7351.
5 A. Zlatanic, C. Lava, W. Zhang and Z. S. Petrovic, Effect of structure on properties of polyols and polyurethanes based on different vegetable oils, *J. Polym. Sci., Part B: Polym. Phys.*, 2004, **42**(5), 809–819.
6 S. Oprea, Effect of the Hard-Segment Structure on the Dielectric Relaxation of Crosslinked Polyurethanes, *J. Appl. Polym. Sci.*, 2011, **119**(4), 2196–2204.
7 S. Oprea, O. Potolinca and V. Oprea, Dielectric properties of castor oil cross-linked polyurethane, *High Perform. Polym.*, 2011, **23**(1), 49–58.
8 D. S. Huh and S. L. Cooper, Dynamic Mechanical Properties of Polyurethane Block Polymers, *Polym. Eng. Sci.*, 1971, **11**(5), 369–376.
9 J. T. Koberstein and R. S. Stein, Small-Angle X-Ray-Scattering Studies of Microdomain Structure in Segmented Polyurethane Elastomers, *J. Polym. Sci., Polym. Phys. Ed.*, 1983, **21**(8), 1439–1472.
10 C. S. Paiksung and N. S. Schneider, Infrared Studies of Hydrogen-Bonding in Toluene Diisocyanate Based Polyurethanes, *Macromolecules*, 1975, **8**(1), 68–73.
11 N. S. Schneider and C. S. Paiksung, Transition Behavior and Phase Segregation in Tdi Polyurethanes, *Polym. Eng. Sci.*, 1977, **17**(2), 73–80.
12 R. W. Seymour and S. L. Cooper, Thermal-Analysis of Polyurethane Block Polymers, *Macromolecules*, 1973, **6**(1), 48–53.
13 R. W. Seymour, G. M. Estes and S. L. Cooper, Infrared Studies of Segmented Polyurethan Elastomers. 1. Hydrogen Bonding, *Macromolecules*, 1970, **3**(5), 579–583.
14 C. H. Y. Chen, R. M. Briber, E. L. Thomas, M. Xu and W. J. Macknight, Structure and Morphology of Segmented Polyurethanes. 2. Influence of Reactant Incompatibility, *Polymer*, 1983, **24**(10), 1333–1340.
15 A. Aneja and G. L. Wilkes, A systematic series of 'model' PTMO based segmented polyurethanes reinvestigated using atomic force microscopy, *Polymer*, 2003, **44**(23), 7221–7228.
16 G. Kacar, E. A. J. F. Peters and G. de With, Mesoscopic simulations for the molecular and network structure of a thermoset polymer, *Soft Matter*, 2013, **9**(24), 5785–5793.
17 G. Kacar, E. A. J. F. Peters and G. de With, Structure of a Thermoset Polymer Near an Alumina Substrate as Studied by Dissipative Particle Dynamics, *J. Phys. Chem. C*, 2013, **117**(37), 19038–19047.
18 G. Kacar, E. A. J. F. Peters and G. de With, Multi-scale simulations for predicting material properties of a cross-linked polymer, *Comput. Mater. Sci.*, 2015, **102**, 68–77.
19 A. C. C. Esteves, K. Lyakhova, L. G. J. van der Ven, R. A. T. M. Benthem and G. de With, Surface Segregation of Low Surface Energy Polymeric Dangling Chains in a Cross-Linked Polymer Network Investigated by a Combined Experimental-Simulation Approach, *Macromolecules*, 2013, **46**(5), 1993–2002.
20 A. C. C. Esteves, K. Lyakhova, J. M. van Riel, L. G. J. van der Ven, R. A. T. M. van Benthem and G. de With, Self-replenishing ability of cross-linked low surface energy polymer films investigated by a complementary experimental-simulation approach, *J. Chem. Phys.*, 2014, **140**(12), 124902.
21 K. Lyakhova, A. C. C. Esteves, M. W. P. van de Put, L. G. J. van der Ven, R. A. T. M. van Benthem and G. de With, Simulation–Experimental Approach to Investigate the Role of Interfaces in Self-Replenishing Composite Coatings, *Adv. Mater. Interfaces*, 2014, **1**(3), 1400053.
22 A. G. Nurioglu, A. C. C. Esteves and G. de With, Non-toxic, non-biocide-release antifouling coatings based on molecular structure design for marine applications, *J. Mater. Chem. B*, 2015, **3**, 6547–6570.
23 R. D. Groot and P. B. Warren, Dissipative particle dynamics: Bridging the gap between atomistic and mesoscopic simulation, *J. Chem. Phys.*, 1997, **107**(11), 4423–4435.
24 P. Espanol, Hydrodynamics from Dissipative Particle Dynamics, *Phys. Rev. E: Stat. Phys., Plasmas, Fluids, Relat. Interdiscip. Top.*, 1995, **52**(2), 1734–1742.
25 P. Espanol and P. Warren, Statistical-Mechanics of Dissipative Particle Dynamics, *Europhys. Lett.*, 1995, **30**(4), 191–196.
26 D. Frenkel and B. Smit, *Understanding Molecular Simulation: From Algorithms to Applications*, Academic Press, California, London, 2002.

27 D. W. van Krevelen and K. ten Nijenhuis, *Properties of polymers: their correlation with chemical structure: their numerical estimation and prediction from additive group contributions*, 4th, completely rev. edn, Elsevier, Amsterdam, 2009.
28 S. Plimpton, Fast Parallel Algorithms for Short-Range Molecular-Dynamics, *J. Comput. Phys.*, 1995, **117**(1), 1–19.
29 H. Makki, K. N. S. Adema, E. A. J. F. Peters, J. Laven, L. G. J. van der Ven, R. A. T. M. van Benthem and G. de With, A simulation approach to study photo-degradation processes of polymeric coatings, *Polym. Degrad. Stab.*, 2014, **105**, 68–79.
30 C. H. Rycroft, VORO++: a three-dimensional voronoi cell library in C++, *Chaos*, 2009, **19**(4), 041111.
31 G. Frenning, Efficient Voronoi volume estimation for DEM simulations of granular materials under confined conditions, *MethodsX*, 2015, **2**, 79–90.
32 V. S. Kumar and V. Kumaran, Voronoi cell volume distribution and configurational entropy of hard-spheres, *J. Chem. Phys.*, 2005, **123**(11), 114501.
33 K. Laidler, *Chemical Kinetics*, TATA McGraw-Hil Publishing Company, New Delhi, 1973.
34 J. H. Ward, K. Furman and N. A. Peppas, Effect of monomer type and dangling end size on polymer network synthesis, *J. Appl. Polym. Sci.*, 2003, **89**(13), 3506–3519.
35 K. Dusek and J. Somvarsky, Chemical clusters in polymer networks, *Faraday Discuss.*, 1995, **101**, 147–158.
36 K. Kojio, M. Furukawa, S. Matsumura, S. Motokucho, T. Osajima and K. Yoshinaga, The effect of cross-linking density and dangling chains on surface molecular mobility of network polyurethanes, *Polym. Chem.*, 2012, **3**(8), 2287–2292.

